

Critical behavior of a polydisperse polymer solution as revealed by turbidity

Rio Kita, Kenji Kubota, and Toshiaki Dobashi

Department of Biological and Chemical Engineering, Faculty of Engineering, Gunma University, Kiryu, Gunma 376, Japan

(Received 21 October 1996; revised manuscript received 3 April 1997)

The critical behaviors were examined for polydisperse polystyrene ($M_w/M_n=2.8$, $M_w=23.9\times 10^4$) in cyclohexane in the vicinity of the critical mixing point using turbidity measurement. Here, M_w and M_n are the weight-averaged and number-averaged molecular weights, respectively. The critical exponents were obtained as $\gamma'=1.38\pm 0.05$ for the osmotic compressibility and $\nu'=0.72\pm 0.02$ for the long-range correlation length together with $\xi_0=0.46\pm 0.06$ nm showing a distinct deviation from the three-dimensional Ising values, and are in agreement with Fisher's renormalized exponents. [S1063-651X(97)02609-3]

PACS number(s): 61.25.Hq, 64.60.Fr, 61.41.+e

INTRODUCTION

Critical behaviors of polymer solutions have been studied in terms of the large fluctuations of the order parameter. These behaviors are characterized by the critical exponents. It has been so far ascertained that the critical behaviors of polymer solutions, composed of a polymer having sufficiently narrow molecular weight distribution and a solvent, belong to the same universality class as the three-dimensional Ising model of simple binary liquid mixtures [1–4]. For example, Kojima *et al.* carried out the light scattering experiments for the mixture of polystyrene and cyclohexane near its critical composition and obtained the critical exponent of the isothermal osmotic compressibility $\gamma=1.24\pm 0.01$ and that of the long-range correlation length $\nu=0.62\pm 0.02$ [4]. In fact, these values are consistent with the three-dimensional Ising model values ($\gamma=1.24$ and $\nu=0.63$ [5,6]) and satisfy the scaling relation $\gamma=(2-\eta)\nu$ with η being the correction factor for the correlation function. Most of the experimental studies were performed using polymers that have very narrow molecular weight distributions, and the theoretical studies were also based on monodisperse polymers. However, a molecular weight distribution is intrinsic to polymer systems and its effect should be an important subject not only for the polymer chemistry but also for the polymer physics. Unfortunately, few accurate studies of the critical behaviors of polydisperse polymer systems have been done because of the difficulty (for example) in determining the critical point. Therefore, it is very interesting and desirable to study the critical behaviors of a polydisperse system in which the polydispersity has been well characterized.

Fisher has studied the impurity effect for binary mixtures near the critical point and found that the critical exponents are renormalized as $f_t=f/(1-\alpha)$ by a fluctuation of an impurity (third component), where f_t and f are the renormalized and three-dimensional Ising critical exponents, respectively, and α is the critical exponent of specific heat for the corresponding binary system [7]. In a previous paper, we reported an experimental study of a coexistence curve for the mixture of polydisperse polystyrene in cyclohexane near its critical mixing point, which emphasized the characteristics of a multicomponent system [8]. Polystyrene has a broad molecular weight distribution of $M_w/M_n=2.8$, where M_w and M_n are the weight- and number-averaged molecular

weights, respectively. Critical exponent β' for the shape of the coexistence curve was obtained as 0.363 ± 0.005 , and clearly deviates from the three-dimensional Ising model value of $\beta=0.326$ [5,6]. This result is in agreement with Fisher's renormalized Ising model prediction with almost a full renormalization, $\beta/(1-\alpha)=0.366$ with α being 0.110 [5,6].

Experimental studies of the critical phenomena of liquid mixtures have been often performed by use of light scattering techniques. Multiple scattering is a serious problem in this method for the mixtures that have large differences in the refractive indices of the components [9–11]. It is very difficult to obtain reliable results for the critical exponents, γ and ν , especially very close to the critical point, and to make the difference between f_t and f clear. The mixture of polystyrene and cyclohexane is one of the systems that shows strong multiple scattering near the critical point. The turbidity, however, is free in principle from the problem of multiple scattering, and turbidity measurement is especially advantageous in such cases, because it is the measurement of unscattered (transmitted) light intensity [9]. In fact, it has been well ascertained that the critical exponents obtained from turbidity measurements are in good agreement with the results of light scattering studies in a simple binary liquid mixture [11], in a cationic surfactant in aqueous salt solution [12], and in a polymer blend [13].

In this paper, we report turbidity measurements of a polydisperse polystyrene solution in cyclohexane near the critical point. We found that the critical behavior of the polydisperse polymer system is characterized by Fisher's renormalized Ising model.

EXPERIMENT

Polystyrene is Styron 666 obtained from Asahi Chemical Industry Co. Ltd., Tokyo, Japan. Its weight-averaged and number-averaged molecular weights are $M_w=23.9\times 10^4$ and $M_n=8.6\times 10^4$, respectively. The molecular weight distribution was characterized by GPC measurements [14], and the shape of the distribution function of the molecular weight is expressed well by a Schulz-Zimm-type distribution [15]. Cyclohexane of reagent grade was distilled twice after being passed through silica gel. No impurity was detected by gas chromatography.

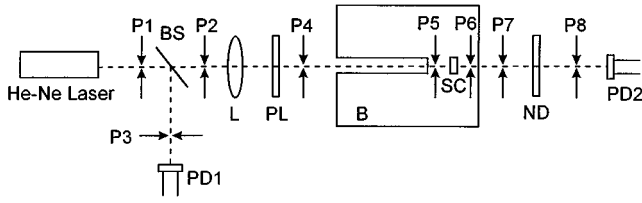


FIG. 1. Schematic diagram of experimental setup of turbidity measurement. P1–P8: pinhole; BS: beam splitter; L: lens; PL: polarizer; B: water bath; SC: sample cell; ND: neutral density filter; PD1 and PD2: photodiode.

For turbidity measurements, a sample solution of the critical concentration, which was determined from the intersection of the coexistence curve and the cloud point curve [8], was prepared in a dry box under dry nitrogen atmosphere and put into a rectangular cell with an optical path length of 5 mm by passing it through a membrane filter (Fluoropore, 0.22 μm of pore size). The sample cell was then flame sealed. The criticality was ascertained by the observation that it separated into two phases with equal volume just below the phase separation temperature (a few mK). Figure 1 shows the experimental setup used in the present study. A He-Ne laser beam operated at a wavelength of 632.8 nm (intensity less than 1 mW) passed through pinholes, a beam splitter, a convex lens, the sample cell and a neutral density filter, and was detected by a photodiode (Hamamatsu Co. Ltd., S1226). The intensity of the incident beam was monitored by another photodiode assembly. The pinholes were used to minimize the effect of unnecessary reflections and to avoid the scattered light. Special care was taken so that the transmitted beam should not be contaminated by the reflections from the

interfaces of optical parts (lens, window, and sample cell). The sample cell was immersed in a water bath, the temperature of which was monitored by a quartz thermometer and controlled within ± 1 mK. Near the critical point $T - T_c < 0.03$ K, the temperature was carefully monitored and controlled within ± 0.2 mK. Water in the bath was thoroughly cleaned by being circulated through a membrane filter of 0.5 μm , before use, to avoid the unnecessary scattering. After changing the temperature, the sample was allowed to accomplish a thorough equilibrium for at least 1 h. The temperature was changed within a few mK near the critical point, and the sample was kept at the same temperature for more than 2 h. The turbidity was determined by measuring both the incident and transmitted (unscattered) light intensities. The errors of turbidity for the respective data points are tabulated in Table I.

Figure 2 shows a schematic phase diagram of the present system. The critical temperature T_c and the critical volume fraction ϕ_c were obtained as $T_c = 26.23$ $^{\circ}\text{C}$ and $\phi_c = 0.0694$, respectively [8]. Solid and broken curves indicate the coexistence curve and the cloud point curve, respectively, and the discrepancy between them is the unique characteristics of a polydisperse polymer solution. The arrow shows the experimental course in the present turbidity measurements.

Turbidity

Turbidity τ is defined as the attenuation of transmitted light intensity per a unit optical length in the medium. When the sample does not absorb the incident beam, the turbidity results from the attenuation due to the scattering. Using the Ornstein-Zernike scattering function in the critical region, τ can be expressed as [9]

TABLE I. Turbidity τ of polydisperse polystyrene in cyclohexane as a function of the reduced temperature ϵ . $\delta\tau$ means the experimental error of τ .

ϵ	τ (cm^{-1})	$\delta\tau^a$ (cm^{-1})	ϵ	τ (cm^{-1})	$\delta\tau^a$ (cm^{-1})
2.3×10^{-6}	3.03	0.03 ₃	2.907×10^{-4}	1.07	0.01 ₉
9.0×10^{-6}	2.64	0.02 ₉	3.341×10^{-4}	1.03	0.01 ₉
1.44×10^{-5}	2.49	0.02 ₈	3.876×10^{-4}	0.95	0.01 ₈
2.91×10^{-5}	2.18	0.02 ₅	4.444×10^{-4}	0.89	0.01 ₈
3.71×10^{-5}	2.05	0.02 ₄	5.379×10^{-4}	0.81	0.01 ₈
4.11×10^{-5}	2.00	0.02 ₄	6.348×10^{-4}	0.74	0.01 ₇
5.75×10^{-5}	1.84	0.02 ₃	7.417×10^{-4}	0.67	0.01 ₇
7.78×10^{-5}	1.70	0.02 ₂	8.754×10^{-4}	0.57	0.01 ₇
8.79×10^{-5}	1.65	0.02 ₂	1.002×10^{-3}	0.52	0.01 ₇
9.56×10^{-5}	1.60	0.02 ₁	1.173×10^{-3}	0.46	0.01 ₆
1.002×10^{-4}	1.59	0.02 ₁	1.377×10^{-3}	0.40	0.01 ₆
1.136×10^{-4}	1.53	0.02 ₁	1.671×10^{-3}	0.34	0.01 ₆
1.303×10^{-4}	1.46	0.02 ₁	1.965×10^{-3}	0.29	0.01 ₆
1.403×10^{-4}	1.42	0.02 ₀	2.399×10^{-3}	0.24	0.01 ₆
1.570×10^{-4}	1.35	0.02 ₀	2.880×10^{-3}	0.20	0.01 ₆
1.771×10^{-4}	1.32	0.02 ₀	3.421×10^{-3}	0.17	0.01 ₆
1.971×10^{-4}	1.28	0.02 ₀	4.126×10^{-3}	0.15	0.01 ₅
2.205×10^{-4}	1.20	0.01 ₉	4.948×10^{-3}	0.12	0.01 ₅
2.606×10^{-4}	1.12	0.01 ₉	5.847×10^{-3}	0.11	0.01 ₅

^a $\delta\tau$ is estimated from the relation of $|\delta\tau| = |\delta I_t/I_t| + |\delta I_0/I_0|$, where I_t and I_0 denote the intensities of the transmitted and incident beam, respectively. It should be noted that the error of the incident beam includes effectively the uncertainty of the background correction.

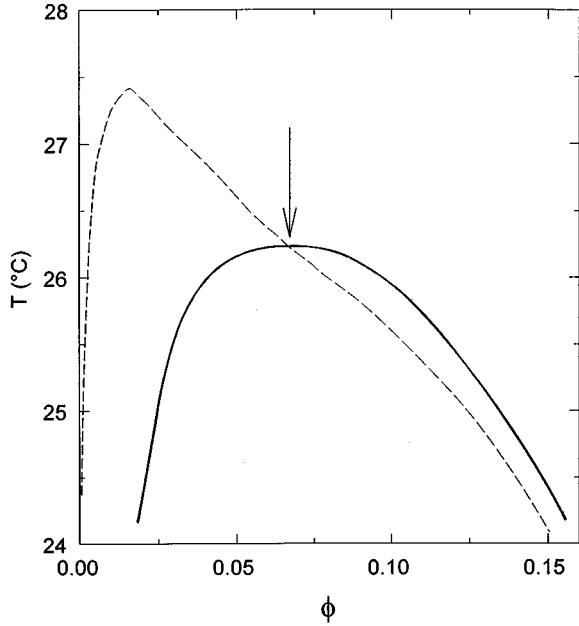


FIG. 2. Schematic phase diagram of polydisperse polystyrene in cyclohexane. Solid and broken curves indicate the coexistence curve and cloud point curve, respectively (see Ref. [8]). The arrow shows the experimental course of the present turbidity measurement.

$$\tau = A_0 T \chi_T G(z), \quad (1)$$

where

$$G(z) = [(2z^2 + 2z + 1)/z^3] \ln(1 + 2z) - 2(1 + z)/z^2, \quad (2)$$

$$z = 2(q_0 \xi)^2. \quad (3)$$

A_0 can be treated as a constant, insensitive to temperature, χ_T is the isothermal osmotic compressibility, ξ is the correlation length, and q_0 is the incident wave vector ($= 2\pi n/\lambda_0$). T , λ_0 , and n are the temperature, wavelength of light in vacuum, and refractive index, respectively. χ_T and ξ are expressed by the following scaling equations:

$$\chi_T = \chi_{T,0} \epsilon^{-\gamma'}, \quad (4)$$

$$\xi = \xi_0 \epsilon^{-\nu'}, \quad (5)$$

where γ' and ν' are the critical exponents of χ_T and ξ , respectively. ϵ is the reduced temperature defined as $\epsilon = (T - T_c)/T_c$.

The turbidity of polymer solutions includes a background part τ_B as well as a net singular part due to the critical phenomena, as demonstrated in several literatures [16,17]. Thus, we used the value $\tau - \tau_B$ as the turbidity in Eq. (1). Here, τ_B was determined by the measurements of turbidity at temperatures far from T_c ($T - T_c = 25$ K). The refractive index of the critical solution, $n = 1.44$, was used to calculate q_0 in Eq. (3).

RESULTS AND DISCUSSION

Figure 3 shows a double-logarithmic plot of turbidity as a function of the reduced temperature ϵ . The numerical data

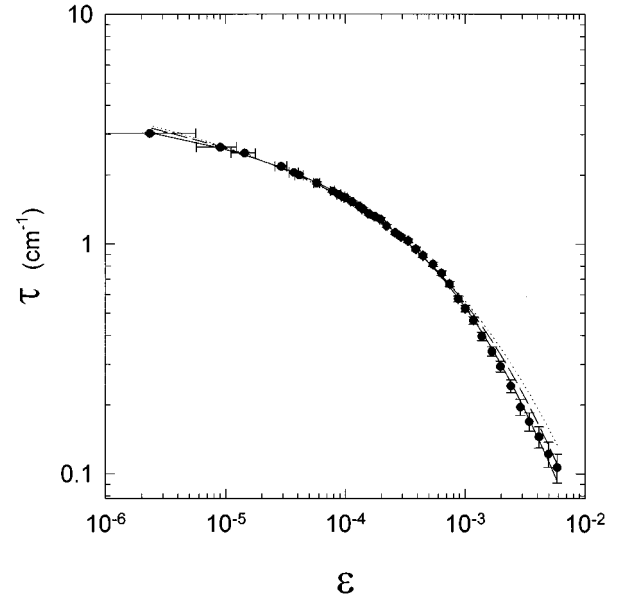


FIG. 3. Double-logarithmic plot of turbidity as a function of the reduced temperature ϵ . The solid, dotted, and dashed curves are the calculated turbidity by Eq. (1) for the four-parameter fit, fixed-fit at Ising values, and fixed fit at fully renormalized values, respectively.

are tabulated in Table I. Turbidity was large ($\tau \sim 3$ at $\epsilon \sim 2 \times 10^{-6}$), suggesting a strong multiple scattering. The critical exponents γ' and ν' were simultaneously determined using a nonlinear least-squares fit (without weighting factors for the fit) to Eq. (1) together with A_0 and ξ_0 . No noticeable systematic deviation was observed over the entire temperature range ($2 \times 10^{-6} < \epsilon < 6 \times 10^{-3}$). The resultant values are $\gamma' = 1.36 \pm 0.05$ and $\nu' = 0.71 \pm 0.02$ together with $\xi_0 = 0.47 \pm 0.06$ nm and $A_0 \chi_{T,0} = (0.40 \pm 0.05) \times 10^{-7}$ (\pm means one standard deviation). The reduced chi square χ_ν^2 was 0.66. A value of χ_ν^2 less than 1 is due to a little overestimation of the experimental error of turbidity measurements. This ξ_0 value is comparable with the reported value $\xi_0 = 0.58$ nm for the binary (monodisperse) polystyrene in cyclohexane obtained by the light scattering measurement [4]. These exponent values are definitely larger than the three-dimensional Ising ones for the binary systems $\gamma = 1.24$ and $\nu = 0.63$, and are in good agreement with the theoretical predictions of Fisher's (fully) renormalized Ising model $\gamma_t = \gamma/(1 - \alpha) = 1.39$ and $\nu_t = \nu/(1 - \alpha) = 0.71$ using $\alpha = 0.110$ [5,6]. The turbidity equations (1)–(3) are complicated and involve interdependent parameters. In such cases, the fits on a parameter should be carefully checked to ensure convincing results. We took an account of the difference of the experimental error of each point and introduced the weighting factors to a fit. The relative deviations from the fitted curve are shown in Fig. 3. No systematic deviation was observed again over the entire temperature range. In this fitting procedure, we tried to use several choices of the initial trial values for the fitting parameters. Those are tabulated in Table II. Although all of the values obtained by the respective fitting are within one standard deviation of each other and the resultant values of χ_ν^2 were essentially the same, a slight dependence on the initial values only for γ' and $A_0 \chi_{T,0}$ were

TABLE II. List of the parameters obtained by the least-squares fit. The values in the parentheses are the fixed values in the fitting and the values in the brackets are the initial trial values in the fitting. \pm indicates standard deviation. The *average values for the four-parameters weighted fit are indicated below their respective columns. Finally, we used the *average values as the starting values. The results are shown in the last row.

	$10^7 A_0 \chi_{T,0}$ ($\text{cm}^{-1} \text{K}^{-1}$)	ξ_0 (nm)	γ'	ν'	χ_ν^2
Unweighted fit					
4 parameters	0.40 ± 0.05	0.47 ± 0.06	1.36 ± 0.05	0.71 ± 0.02	0.66
Ising	1.21 ± 0.07	1.05 ± 0.05	(1.24)	(0.63)	8.26
Fully renormalized	0.43 ± 0.02	0.63 ± 0.02	(1.39)	(0.71)	3.65
Weighted fit					
4 parameters	0.33 ± 0.10	0.44 ± 0.06	1.39 ± 0.05	0.73 ± 0.02	0.67
Ising	1.13 ± 0.06	1.00 ± 0.04	(1.24)	(0.63)	7.09
	0.77 ± 0.02	0.57 ± 0.02	(1.24)	0.66 ± 0.02	0.76
	1.14 ± 0.02	0.64 ± 0.02	1.17 ± 0.04	(0.63)	0.92
Fully renormalized	0.42 ± 0.02	0.62 ± 0.02	(1.39)	(0.71)	2.86
	0.33 ± 0.01	0.44 ± 0.02	(1.39)	0.73 ± 0.01	0.63
	0.41 ± 0.01	0.47 ± 0.02	1.35 ± 0.01	(0.71)	0.64
Weighted fit					
	0.47 ± 0.14 [1.13]	0.50 ± 0.06 [1.00]	1.33 ± 0.05 [1.24]	0.70 ± 0.02 [0.63]	0.68
	0.35 ± 0.11 [1.13]	0.45 ± 0.06 [1.00]	1.38 ± 0.05 [1.39]	0.72 ± 0.02 [0.71]	0.65
	0.44 ± 0.13 [0.42]	0.48 ± 0.06 [0.62]	1.34 ± 0.05 [1.24]	0.70 ± 0.02 [0.63]	0.67
	0.34 ± 0.10 [0.42]	0.45 ± 0.06 [0.62]	1.39 ± 0.05 [1.39]	0.72 ± 0.02 [0.71]	0.65
*average	0.400	0.470	1.360	0.710	
	0.36 ± 0.11 [0.40]	0.46 ± 0.06 [0.47]	1.38 ± 0.05 [1.36]	0.72 ± 0.02 [0.71]	0.65

observed. Therefore, we adopted the averaged values resulting from those fitting routines as the final initial trial values. The resultant values are $\gamma' = 1.38 \pm 0.05$ and $\nu' = 0.72 \pm 0.02$ together with $\xi_0 = 0.46 \pm 0.06$ nm and $A_0 \chi_{T,0} = (0.36 \pm 0.11) \times 10^{-7}$ ($\chi_\nu^2 = 0.65$). These values agree well with those by the unweighted fit.

Moreover, we tried to use a constrained fit by fixing the critical exponents at the theoretical values for Ising values and fully renormalized values. Figure 3 shows systematic deviations from the fits, for both the constrained fits of Ising values and fully renormalized values. The deviations were larger and more systematic for Ising values than for fully renormalized values, as shown in Fig. 4. For weighted and unweighted fits, χ_ν^2 were 7.09 and 8.26, respectively, with Ising values, and 2.86 and 3.65, respectively, with fully renormalized values. The parameters determined by the statistical analyses were listed in Table II. Least-squares fits using fixed values for the exponents showed large systematic deviations and large χ_ν^2 , especially for Ising values. Constrained fits (with fixing only one of the critical exponents at the theoretical values) for Ising values and fully renormalized values were also examined (see Table II). The cases of fixing for the Ising value are not good, and fixing at the fully renormalized value gives almost the same result as those of the four-parameter fit. The four-parameter fit (with no constraint) showed reasonably small χ_ν^2 and no systematic deviation. A difference of χ_ν^2 between the four-parameters fit and the fixed fit at fully renormalized values is attributable to the small difference of the exponents, since the fitting is significantly affected by the exponent values. In Fig. 4 the deviation of the closest point to T_c is very large for the

constrained fit for Ising exponents (triangles) and for fully renormalized exponents (squares). Then, we tried to analyze the data when omitting this point. The resultant parameters were essentially the same as those listed in Table II. These

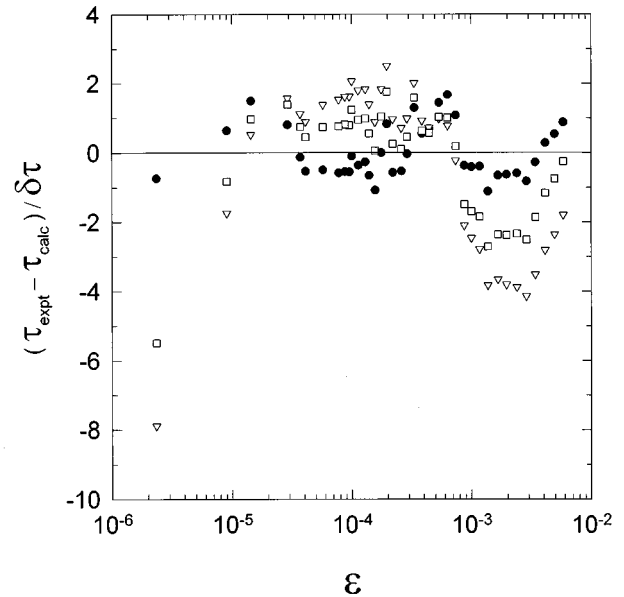


FIG. 4. Relative deviations as a function of the reduced temperature ϵ . τ_{expt} is the observed turbidity and τ_{calc} is the calculated turbidity with Eq. (1) using values for the four-parameters fit (●), fixed-fit at Ising exponents (▽), and fixed-fit at fully renormalized exponents (□). $\delta\tau$ means the error of turbidity for the respective points.

analyses clearly show that the critical behavior of the present system revealed by turbidity is expressed well by the renormalized Ising values excluding the Ising values.

In our previous paper, we found $\beta' = 0.363 \pm 0.005$, indicating a good consistency with the present values. The present results again ascertained that the critical behaviors of a polydisperse polymer solution are expressed well by Fisher's fully renormalized Ising model, as well as bimodal polymer solutions and ternary mixtures. Moreover, these exponents satisfy the scaling relations of $\alpha' = 2 - d\nu' = 2 - 3 \times 0.72 = -0.16 \pm 0.04$ and $\alpha' + 2\beta'\gamma' = -0.16 + 2 \times 0.363 + 1.38 = 1.95 \pm 0.10$ in agreement with a negative value of α' corresponding to $\alpha = 0.11$ [5,6].

Broseta and Leibler studied the critical behavior of a bimodal polymer solution and showed that Fisher's renormalization becomes visible at the critical value $\epsilon^* < k^{1/\alpha}$, where k is related to the volume fraction of a polymer with a larger molecular weight in the total polymer and to the molecular weight ratio of two polymer components [18]. Because of the large power of $1/\alpha$, such a crossover could be realized even with the addition of a small amount of a higher molecular weight component. This point has already been experimentally observed for the system of two homologous polymers in a solvent (polystyrene I + polystyrene II + methylcyclohexane) [19,20]. The interaction that governs the dominant fluctuation relating to the critical behaviors is modulated by the coexisting impurity, and critical behaviors due to such a modulation could be expressed by the universal manner of Fisher's renormalization. According to this viewpoint, the critical behaviors of a polydisperse system correspond to those of a ternary system when its polydispersity is large enough. In the present case, polydispersity works to modulate the interaction.

Experimental studies of the impurity effect on the critical phenomena in binary fluid mixtures have been carried out for systems with a variety of impurities along various thermodynamic paths. Bak and Goldberg found that the enhanced values of critical exponents γ and ν could be observed in the systems with large enough amounts of impurities [21,22]. Jacobs and his colleagues showed a linear dependence of β on the amount of impurities for a binary system of methanol + cyclohexane [23,24]. Fisher's fully renormalized

exponents β' , γ' , and ν' have been verified for ordinary ternary mixtures, e.g., ethanol + chloroform + water [25–29]. In bimodal polymer solutions, a large amount of a higher molecular weight component and a high molecular weight ratio of the two polymers were considered to raise the visibility of the renormalized exponents [18–20]. Binary and ternary polymer blends also showed the renormalization of the critical exponents [30,31]. In the former case, it is believed that a large amount of free volume change on mixing may be the cause of the impurity effect, which results in the renormalization of the critical exponents [30]. Recently, the evidence for renormalization was also demonstrated in more complex systems, such as micelles and microemulsions, which may be regarded as quasiternary systems, although there still remains some controversial problems [12,32–35]. The type of the impurity in the present multicomponent system, a polydisperse polymer with a wide molecular weight distribution in a solvent, is very different from those studied so far. Agreement of the critical exponents in the present system with other systems indicates a universality of the impurity effect on the critical behaviors of binary fluid mixtures.

Tanaka recently proposed the concept that the topological characteristics of the polymer chain induce a kinetic coupling between the stress field and the order parameter in polymer solution dynamics [36]. Since this mechanism is brought about by the asymmetry in molecular dynamics of polymer and solvent, the molecular weight distribution should give essential effects on this phenomena. It is interesting to study critical dynamics and phase separation in relating to such a novel concept, using a well characterized polymer as the extension of this work.

ACKNOWLEDGMENTS

The authors are grateful to Professor K. Kamide of Kumamoto University for providing us the polystyrene sample and M. Yoneyama of Gunma University for his help in gas chromatography measurements. We wish to acknowledge the support of a grant-in-aid from the Ministry of Education, Science, and Culture of Japan, and R. K. wishes to thank JSPS for financial support.

-
- [1] H. E. Stanley, *Introduction to Phase Transitions and Critical Phenomena* (Oxford University Press, London, 1972).
- [2] Q. H. Lao, B. Chu, and N. Kuwahara, *J. Chem. Phys.* **62**, 2039 (1975).
- [3] M. Nakata, N. Kuwahara, and M. Kaneko, *J. Chem. Phys.* **62**, 4278 (1975).
- [4] J. Kojima, N. Kuwahara, and M. Kaneko, *J. Chem. Phys.* **63**, 333 (1975).
- [5] A. J. Liu and M. E. Fisher, *Physica A* **156**, 35 (1989).
- [6] J. V. Sengers and J. M. H. L. Sengers, *Annu. Rev. Phys. Chem.* **37**, 189 (1986).
- [7] M. E. Fisher, *Phys. Rev.* **176**, 257 (1968).
- [8] R. Kita, T. Dobashi, T. Yamamoto, M. Nakata, and K. Kamide, *Phys. Rev. E* **55**, 3159 (1997).
- [9] V. G. Puglielli and N. C. Ford, Jr., *Phys. Rev. Lett.* **25**, 143 (1970).
- [10] J. G. Shanks and J. V. Sengers, *Phys. Rev. A* **38**, 885 (1988).
- [11] K. Hamano, S. Teshigawara, T. Koyama, and N. Kuwahara, *Phys. Rev. A* **33**, 485 (1986).
- [12] K. Kubota, N. Kuwahara, and H. Sato, *J. Chem. Phys.* **100**, 4543 (1994).
- [13] H. Sato, N. Kuwahara, and K. Kubota, *Phys. Rev. E* **53**, 3854 (1996).
- [14] K. Kamide, K. Sugamiya, T. Ogawa, C. Nakayama, and N. Baba, *Makromol. Chem.* **135**, 23 (1970); K. Kamide, S. Matsuda, T. Dobashi, and M. Kaneko, *Polym. J.* **16**, 839 (1984).
- [15] G. V. Schulz, *Z. Phys. Chem. Abt. B* **43**, 25 (1939); **44**, 227 (1939); B. H. Zimm, *J. Chem. Phys.* **16**, 1099 (1948).

- [16] W. Shen, G. R. Smith, C. M. Knobler, and R. L. Scott, *J. Phys. Chem.* **95**, 3376 (1991).
- [17] T. Narayanan and K. S. Pizer, *J. Chem. Phys.* **102**, 8118 (1995).
- [18] D. Broseta and L. Leibler, *J. Chem. Phys.* **90**, 6652 (1989).
- [19] T. Dobashi and M. Nakata, *J. Chem. Phys.* **101**, 3390 (1994).
- [20] T. Dobashi, M. Nakata, and M. Kaneko, *J. Chem. Phys.* **80**, 948 (1984).
- [21] C. S. Bak and W. I. Goldberg, *Phys. Rev. Lett.* **23**, 1218 (1969).
- [22] C. S. Bak, W. I. Goldberg, and P. N. Pusey, *Phys. Rev. Lett.* **25**, 1420 (1970).
- [23] J. L. Tveekrem and D. T. Jacobs, *Phys. Rev. A* **27**, 2773 (1983).
- [24] R. H. Cohn and D. T. Jacobs, *J. Chem. Phys.* **80**, 856 (1984).
- [25] J. A. Zollweg, *J. Chem. Phys.* **55**, 1430 (1971).
- [26] L. E. Wold, Jr., G. L. Pruitt, and G. Morrison, *J. Phys. Chem.* **77**, 1572 (1973).
- [27] B. Chu and F. L. Lin, *J. Chem. Phys.* **61**, 5132 (1974).
- [28] K. Ohbayashi and B. Chu, *J. Chem. Phys.* **68**, 5066 (1978).
- [29] S. J. Rzoska and J. Chrapek, *J. Chem. Phys.* **90**, 2783 (1989).
- [30] D. Schwahn, H. Takeno, L. Willner, H. Hasegawa, H. Jinnai, T. Hashimoto, and M. Imai, *Phys. Rev. Lett.* **73**, 3427 (1994).
- [31] H. Yajima, D. W. Hair, A. I. Nakatani, J. F. Douglas, and C. C. Han, *Phys. Rev. B* **47**, 12 268 (1993).
- [32] M. W. Kim, J. Bock, and J. S. Huang, *Phys. Rev. Lett.* **54**, 46 (1985).
- [33] P. Honorat, D. Roux, and A. M. Bellocq, *J. Phys. (France) Lett.* **45**, L961 (1984).
- [34] Y. Jayalakshmi and D. Beysens, *Phys. Rev. A* **45**, 8709 (1992).
- [35] R. Aschauer and D. Beysens, *Phys. Rev. E* **47**, 1850 (1993).
- [36] H. Tanaka, *J. Chem. Phys.* **100**, 5323 (1994).